



Phosphate adsorption characteristics of wasted low-grade iron ore with phosphorus used as natural adsorbent for aqueous solution

Xiaoli Yuan^{a,b}, Chenguang Bai^a, Wentang Xia^{b,*}, Bing Xie^a, Juan An^b

^aCollege of Material Science and Engineering, Chongqing University, Chongqing 400044, China

^bSchool of Metallurgy and Material Engineering, Chongqing University of Science and Technology, Chongqing 401331, China, Tel./Fax: +86 23 65023436; email: wentangx@163.com

Received 7 September 2013; Accepted 14 March 2014

ABSTRACT

A low-grade iron ore with phosphorus (LGIOWP), the extensive industrial solid waste generated in mining of high phosphorus iron ore, was investigated to assess the effectiveness for the removal of phosphate from aqueous solution. The factors influencing the adsorption were examined, and the related adsorption mechanism was discussed. The results showed that pH value had a significant effect on the phosphate removal. The optimum pH value for phosphate adsorption was 5.6. The adsorption of phosphate mainly on hematite ligand exchange is likely the key mechanism for phosphate removal when pH is in the range of 1–9. When pH value was above 9, the presence of dolomite played an important role in phosphate removal. The adsorption capacity is enhanced with a higher initial phosphate concentration. Kinetic studies show that the adsorption follow pseudo-second-order kinetic model. Langmuir and Freundlich isotherms were used to simulate the adsorption equilibrium data. The adsorption fits well with the Langmuir isotherm model and the maximum adsorption capacity is found to be 11.44 mg/g. Due to possessing the low cost and high capability, LGIOWP could be a promising material for phosphate removal in the wastewater treatment.

Keywords: Low-grade iron ore with phosphate (LGIOWP); Phosphate removal; Adsorption; Isotherm; Kinetics

1. Introduction

As is well known, phosphorus is an essential nutrient for all life forms on Earth [1]. However, excessive phosphorus in wastewater causes eutrophication, which contributes to the environmental problems. The well-recognized disastrous consequences include the imbalances in aquatic populations, degraded water quality, overpopulated aquatic plants, and disturbance in balance of the organisms presented in water. The

principal phosphorus compounds in wastewater mainly exist as orthophosphates. Consequently, it is necessary to remove phosphate from surface waters in order to avoid any kinds of problems, particularly near urban areas.

Lots of methods have been developed for phosphate removal, such as biological processes [2,3], chemical precipitation [4], adsorption [5], membrane technologies [6], and ion exchange [7]. In these methods, membrane technologies and ion exchange require high cost in initial investment and facility setup and

*Corresponding author.

operation. Since biological processes require highly skillful operation techniques, it is very difficult to operate the process stably in the phosphate removal treatment. Chemical removal techniques are well-established and the most effective methods up to date. However, there is a potentially high cost in coagulating agents and sludge handling [8]. Compared with other techniques, adsorption is cost effective and comparatively handy for phosphate removal. A great attention has been paid to low-cost adsorbents over past years, such as hematite [9], limestone [10], iron oxide tailing [11], ferric sludge [12], iron-based compounds [13], blast furnace slag [14], aluminum-based compounds [15], dolomite [16], layered double hydroxides [17], phosphate mine slimes [18], calcite [19], apatite [20], natural zeolite [21], and other materials. The removal mechanism is mainly either precipitation or adsorption. The major advantage of using these materials or by-products for wastewater treatment is low cost.

Iron ore is the main raw materials of iron and steel industry. However, the high-grade iron ore with low harmful P and S impurity was decreasing gradually with the rapid development of modern industry. More and more nontraditional iron ores with high phosphorus is exploited as a result. High-phosphorus ores became a significant source for the modern iron and steel industry [22]. In mining high-phosphorus iron ores, a large amount of low-grade iron ores with phosphorus (LGIOWP) wastes are generated, which causes a very serious waste disposal problem with the increasing of LGIOWP. Up to now, there is very little work has been carried out regarding the reuse of LGIOWP. So LGIOWP treatment and recycling becomes an urgent worldwide problem to be solved. LGIOWP mainly contains metal oxides (hematite), dolomite, quartz, and silicate. It is well recognized that most of these minerals are useful adsorbent for phosphate removal in aqueous solution [13,16,20]. Unfortunately, no significant research works have been reported on the reuse of LGIOWP for wastewater treatment in general and phosphates removal in particular. In regarding to environmental and economical concerns, it is an effective way to utilize the low-cost LGIOWP to remove phosphate and to ensure that phosphorus resources to be recycled and reused.

The aim of this study was to investigate the feasibility of using LGIOWP as a natural adsorbent for phosphate removal from aqueous solution. The adsorption characteristics of LGIOWP material for phosphate removal from aqueous solution were evaluated. Effects of the key process parameters such as initial pH value, initial phosphate concentration, adsorbent dosage, adsorption time, and adsorption

temperature on the adsorption capacity of phosphate were investigated. In addition, the adsorption kinetics and isotherms behaviors of phosphate removal by LGIOWP were examined.

2. Materials and methods

2.1. Materials

LGIOWP (mass percent, Fe 25.49%, P 1.28%, Ca 14.84%, Si 7.54%, Mg 4.82%), used in this research was obtained from Wushan, Chongqing, China. The ores were crushed and sieved to obtain the adsorbent with particle size less than 0.147 mm. A stock solution of 1,000 mg P/L in orthophosphates was prepared by dissolving a certain amount of chemically pure KH_2PO_4 in deionized water. Phosphate working solutions in different concentrations were prepared by diluting the stock phosphate solution with deionized water. An appropriate volume of 0.1 mol/L HCl and NaOH was used to adjust the pH of the solution.

2.2. Adsorption experiments

Adsorption experiments were carried out as the following procedure. First, a defined volume of phosphate stock solution was diluted to the required concentration by adding deionized water in 100 mL glass round-bottom flasks immersed in a thermostatic shaker bath. The pH value of the solution was then adjusted to the desired value and a defined amount of adsorbent was added. The mixture was stirred at 250 rounds per minute for a defined period, using a stirred with a potentiometer to regulate the stirring speed. Liquid samples were collected at various time intervals and filtering process was applied to separate solid from liquid, and the filtrate was taken for P analysis.

The effect of initial pH on phosphate adsorption was investigated in a series of experiments that maintained pH value in the range 1–13, while fixed the initial phosphate concentration, LGIOWP dosage, adsorption temperature, and adsorption time to 20 mg P/L, 5 g/L, 25 °C, and 1 h, respectively.

The effect of LGIOWP dosage on phosphate adsorption was investigated through experiments with LGIOWP dosage ranging from 2 to 20 g/L, and fixed initial pH value 5.6, initial phosphate concentration 20 mg P/L, adsorption temperature 25 °C, and adsorption time 1 h.

Phosphate adsorption kinetics studies were evaluated with a combination of different adsorption time, different initial phosphate concentrations, fixed LGIOWP dosage (10 g/L), and pH value (5.6) at 25 °C.

Five levels of initial phosphate concentrations (20, 50, 75, 100, and 150 mg P/L) and adsorption time (0.5, 1, 1.5, 2, and 2.5 h) were used. In order to investigate the potential rate-controlling step of the phosphate adsorption process, several kinetics models, such as Elovich model, pseudo-first-order model, intra-particle diffusion model, and pseudo-second-order model were employed to evaluate phosphate adsorption kinetics performance. The following Eqs. (1)–(4) were applied for describing the four kinetics models, respectively [23–26]:

$$\text{Elovich model: } q_t = \frac{1}{\beta \ln(\alpha\beta)} + \frac{1}{\beta} \ln t \quad (1)$$

$$\text{Pseudo-first-order model: } \frac{1}{q_t} = \frac{k_1}{q_e t} + \frac{1}{q_e} \quad (2)$$

$$\text{Intra-particle diffusion model: } q_t = c + k_m t^{1/2} \quad (3)$$

$$\text{Pseudo-second-order model: } \frac{t}{q_t} = \frac{1}{k_2 q_e^2} + \frac{t}{q_e} \quad (4)$$

where t is the contact time of adsorption experiment (h), q_e (mg/g) and q_t (mg/g) are, respectively, the adsorption capacity at equilibrium and at any time t , α is the initial adsorption rate constant (mg/(g·min)) and the parameter β (g/mg) is related to the extent of surface coverage and activation energy for chemisorption, k_1 (min⁻¹) is the rate constant of the pseudo-first-order model, k_m (mg/(g·min^{1/2})) is the rate constant of the intra-particle diffusion model and c is obtained from the intercept, k_2 (g/(mg·min)) is the rate constant of the pseudo-second-order model. The initial adsorption rate is $k_2 q_e^2$ (mg/(g·min)).

The effect of adsorption temperature on phosphate removal and phosphate adsorption isotherms tests was studied at four different temperatures (25, 35, 45, and 55 °C) for 1 h with fixed LGIOWP dosage of 10 g/L and pH value of 5.6, and the initial phosphate concentration varies from 20 to 150 mg P/L. Adsorption isotherms data were evaluated using the Langmuir and Freundlich equations, respectively, expressed in Eqs. (5) and (6) [27,28]:

$$q_e = \frac{q_{\max} K_L C_e}{1 + K_L C_e} \quad (5)$$

$$q_e = K_F C_e^{1/n} \quad (6)$$

The linear equations of these two experiential models are listed as Eqs. (7) and (8):

$$\frac{C_e}{q_e} = \frac{C_e}{q_{\max}} + \frac{1}{K_L q_{\max}} \quad (7)$$

$$\lg q_e = \lg K_F + \frac{\lg C_e}{n} \quad (8)$$

where C_e is the equilibrium concentration of phosphate in the solution (mg/L), q_e is the phosphate concentrations in the solid adsorbent (mg/g), q_{\max} is the maximum adsorption capacity (mg/g), K_L is a constant related to the energy of adsorption (L/g), K_F is a constant related to the adsorption capacity (mg^{1-1/n}L^{1/n}g), and n is a constant related to the energy of adsorption.

2.3. Characterization methods

The pH value of the aqueous solution was measured by pH meter (METTLER-TOLED). The P content of all samples including aqueous solution was analyzed by bismuth-phosphomolybdenum blue spectrophotometric method (Model TU-1810, Beijing Puxi Science and Technology Instrument Co Ltd, China) at λ_{\max} of 700 nm with the blank sample containing only deionized water and corresponding LGIOWP as a reference. Phase analyses of LGIOWP before and after phosphate adsorption were conducted by X-ray diffraction (XRD) (Model D/max 2500 PC, Rigaku, Japan) with Cu K (alpha) radiation. Microstructure of LGIOWP was observed by scanning electron microscopy (SEM) (Model VEGA3, TESCAN, Czech). The particle size distribution and specific surface area of LGIOWP were characterized using nitrogen adsorption BET method by laser diffraction particle size analyzer (Model MS 2000, Malvern, USA).

3. Results and discussion

3.1. Characteristics of LGIOWP

Fig. 1 shows the XRD pattern of LGIOWP. Intensive diffraction peaks of hematite (Fe₂O₃), dolomite (CaMg(CO₃)₂), and quartz (SiO₂) and relatively weak peaks of fluorapatite (Ca₅(PO₄)₃F) were observed in Fig. 1. The XRD results indicate that the crystalline phases present in LGIOWP are mainly hematite, dolomite, and quartz accompanied by a minor amount of fluorapatite. Fig. 2 presented the typical SEM images of LGIOWP powders after being crushed and screened. It can be seen that the LGIOWP particles aggregate to form a porous structure and a rough surface. The powder had an average particle size of 67.3 μm and specific surface area of 2.03 m²/g. In addition, particle size analysis (as shown in Fig. 3) shows a wide distribution of particle

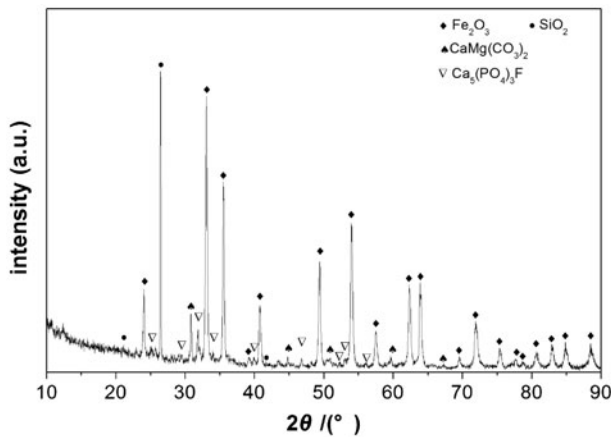


Fig. 1. XRD pattern of LGIOWP.

size i.e. 10.8% less than $1\ \mu\text{m}$, 61.9% between 1 and $100\ \mu\text{m}$ and 27.3% more than $100\ \mu\text{m}$.

3.2. Effect of initial pH value on phosphate adsorption

The pH value of the aqueous solution is considered to be an important variable for the removal of phosphate from aqueous solution. Fig. 4 illustrates the effect of initial pH value on the phosphate adsorption by the LGIOWP for pH values between 1 and 13. As seen from Fig. 4, the phosphate concentration after the reaction emerges to the pattern “W” and the adsorption capacity of phosphate appears to the pattern “M.”

As the pH value increased from 1.74 to 5.6, the phosphate adsorption capacity enhanced, and the phosphate concentration in aqueous solution decreased. When the pH is 5.6, the maximum phosphate adsorption capacity is obtained, and the value is $4.0\ \text{mg/g}$. The phosphate adsorption capacity decreases with the increase of pH when pH locates at the range of 5.6–9, while increases when pH locates at the range of 9–10.67. With the pH further increasing, the phosphate removal efficiency again decreases with pH increasing.

As stated above, the maximum adsorption amount of phosphate appears at pH 5.6 and decreases with either decreasing or increasing initial pH. The similar behavior was also reported for phosphate adsorption on ferric sludge [29] and hematite [9] at the pH ranging from 1 to 9. As mentioned earlier, LGIOWP also contains certain amount of dolomite and quartz. Hence, the actual phosphate removal using LGIOWP as adsorbent could be a consequence of adsorption and precipitation reactions with Fe, Ca, Mg, and Si. However, the chemical precipitation in the forms of calcium phosphates or apatite is favored at pH values above 9 [30]. In addition, previous works reported that the phosphate removal by fixation with Mg^{2+} ions was not accomplished or it was low [31]. Moreover, it is well known that quartz is material with a weak affinity for phosphorus binding [32,33]. Therefore, adsorption of phosphate mainly on hematite is likely the key mechanism for phosphate removal using the present LGIOWP at pH 1–9.

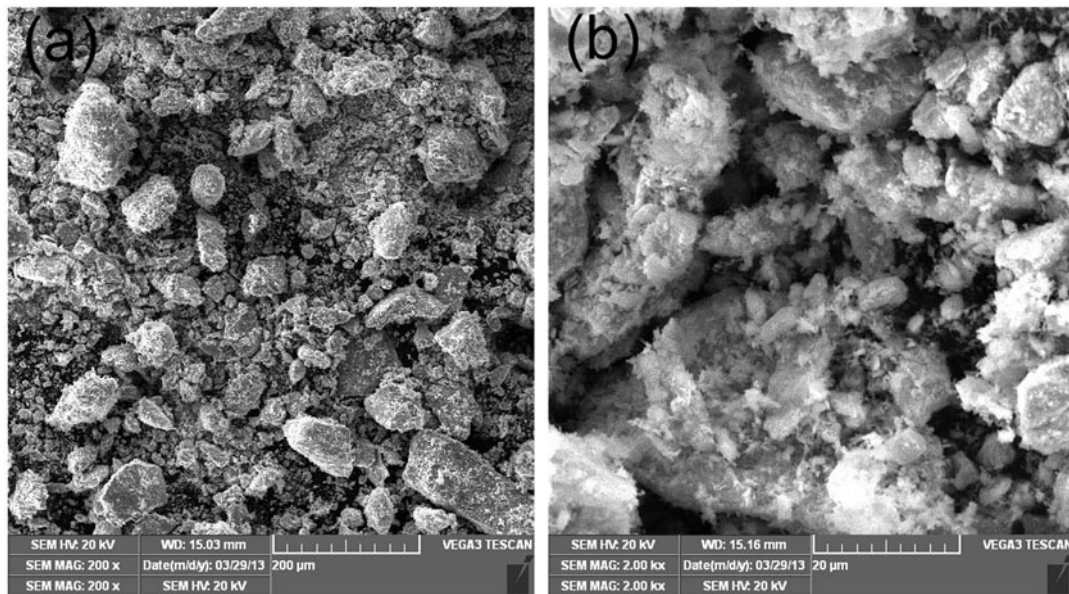


Fig. 2. SEM micrographs of LGIOWP.

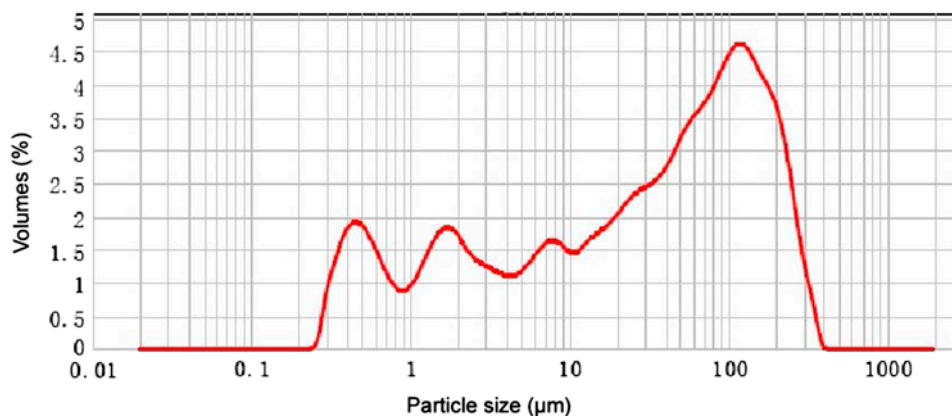


Fig. 3. Particle size distribution of LGIOWP.

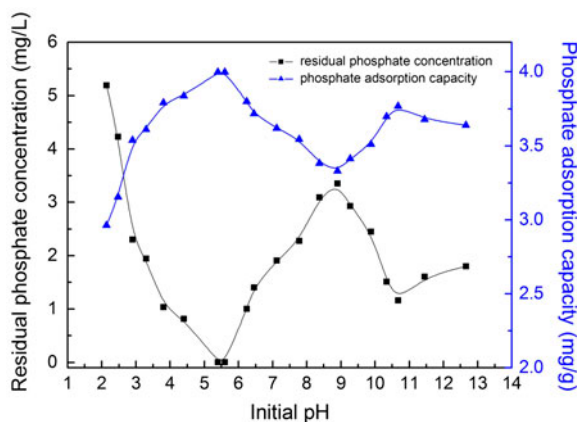
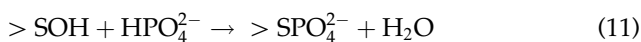


Fig. 4. Effect of pH on phosphate adsorption on LGIOWP.

For KH_2PO_4 solution, three acidic phosphorus species, namely H_3PO_4 , H_2PO_4^- , and HPO_4^{2-} [34], may be expected to dominate between 1 and 9, all of which will be adsorbed on the solid surface. Thus, the adsorption of phosphate at pH in range of 1–9 can be a ligand exchange mechanism described as Eqs. (9)–(11):



Here, $>\text{SOH}$ represents surface hydroxyl groups of LGIOWP (where S refers to a central ion of the mineral surface). As is well known, oxide surfaces in aqueous suspension usually coordinate water molecules. Hence LGIOWP surfaces will be covered by surface hydroxyl groups.

As shown in Fig. 4, LGIOWP exhibits relative high phosphate adsorption capacity at pH 4–6, at which point the predominant phosphate form is H_2PO_4^- , and the mainly formed substance may be SHPO_4^- . The low pH values are advantageous to the phosphate adsorption because of anion adsorption combined with the release of hydroxyl anions [35]. The decrease of phosphate adsorption above pH 5.6 may be due to the fact that a higher pH causes the iron oxide surface to carry more negative charges and thus would more significantly repulse the negatively charged species in solution [36].

It is noteworthy that the phosphate adsorption capacity of LGIOWP enhanced as pH value increased when pH values locates at the range of 9–10.67. Previous studies indicated that Ca^{2+} concentrations in the solution decreased with increased initial pH for different phosphate concentrations [11,37]. Obviously, this trend of LGIOWP suggests that precipitation with Ca should be a significant process responsible for the phosphate removal by the LGIOWP when pH value ranges from 9 to 10.67. When pH is about 10.67, the main P species is HPO_4^{2-} , so dolomite dissolves to emerge partial Ca^{2+} , Ca^{2+} reacts with HPO_4^{2-} to form hydroxylapatite. The above conclusion is confirmed by the XRD pattern at initial pH 10.67. As shown in Fig. 5, weak diffraction peaks of $\text{Ca}_{10}(\text{PO}_4)_6(\text{OH})_2$ appear after adsorption.

3.3. Effect of LGIOWP dosage on phosphate adsorption

To study the effect of LGIOWP dosage on phosphate adsorption efficiency, some adsorption experiments were carried out accordingly and the results were shown in Fig. 6. The results indicate that the LGIOWP dosage has a great influence on phosphate

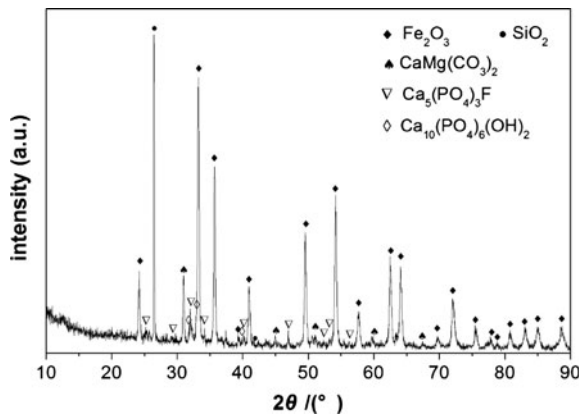


Fig. 5. XRD pattern of LGIOWP after adsorption at initial pH 10.67.

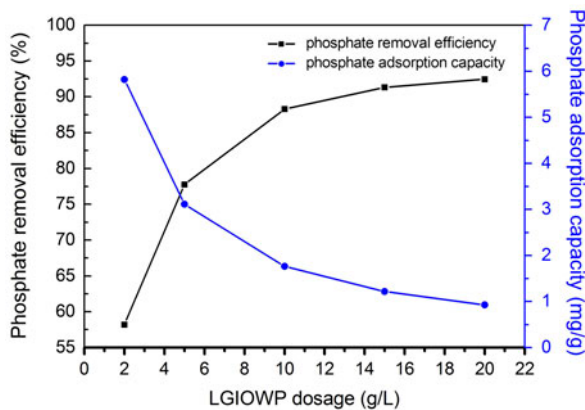


Fig. 6. Effect of LGIOWP dosage on phosphate adsorption.

adsorption. As seen from Fig. 6, the value of phosphate adsorption capacity decreased, but the removal efficiency of phosphate increased from 58.2 to 88.3% with an increase in amount of adsorbent up to 10 g/L. It is explained that more active sites are available for the phosphate binding with the addition of more adsorbent. However, the phosphate removal rate was fairly constant when the LGIOWP dosage was greater than 10 g/L with a continuous decrease in phosphate adsorption capacity. Therefore, it is suggested that the optimal adsorbent dosage was 10 g/L in subsequent experiments.

3.4. Effect of initial phosphate concentration

The effect of initial phosphate concentration on the adsorption capacity (q_t) of LGIOWP is shown in Fig. 7. It can be seen that the adsorption capacity of LGIOWP increased with increase in the initial phosphate con-

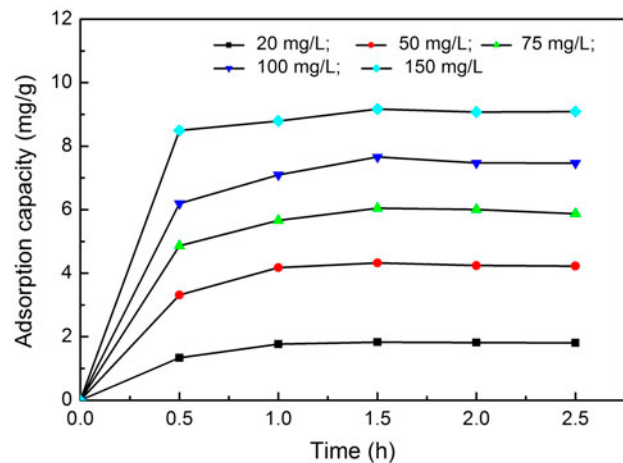


Fig. 7. The variation of adsorption capacity of LGIOWP with adsorption time at various initial phosphate concentrations.

centration. The adsorption saturation time was 1 h for all initial concentrations studied. The adsorption capacity remains nearly constant after adsorption saturation. It also shows that the adsorption rate is rapid in the initial stages (0–1 h) and gradually decreases with progress of adsorption for all different initial phosphate concentrations. In addition, it is interesting to find that the adsorption capacity (q_t) of the sample with a relative low initial phosphate concentration exhibit a more abrupt increasing tendency when the adsorption time is extended from 0 to 0.5 h, the adsorption capacity (q_t) values of phosphate increases by 32.18, 25.94, 16.45, 14.53, 3.53% for the initial phosphate concentrations of 20, 50, 75, 100, and 150 mg/L, respectively.

3.5. Phosphate adsorption kinetics

It can be seen that the adsorption process could be divided into two distinctive sections ($t < 1$ h and $t > 1$ h) from the results of phosphate adsorption kinetics experiments with different initial phosphate concentrations as shown in Fig. 7. This kinetics experiments clearly indicate that adsorption of phosphate ion on LGIOWP is a two-step process similar to experiments by previous studies [37–39]: A rapid adsorption of phosphate ion to the external surface is followed by the possible slow intra-particle diffusion in the interior of the adsorbent. This two-stage phosphate ion uptake can be explained as adsorption occurring onto two different types of binding sites on the adsorbent particles. The rapid kinetics has significant practical importance, as it facilitates smaller reactor volumes, and ensures higher efficiency and economy [40].

The fitting of the experimental data to the linear forms of the four adsorption kinetics models (Eqs. (1)–(4)) were shown in Fig. 8(a)–(d), respectively. In addition, the corresponding rate constants and parameters were listed in Table 1. Obviously, the Elovich, pseudo-first-order and intra-particle diffusion kinetic models were ruled out because their correlation coefficients (R^2) for the present experimental data were too small (<0.9). It can be seen that the experimental data fit well with the pseudo-second-order model with a high R^2 of 0.9969–0.9999. These results indicate that the adsorption system studied satisfied the pseudo-second-order kinetic model. Also, this suggests the assumption behind the pseudo-second-order model that the phosphate ion uptake process is due to chemisorptions [41]. Similar phenomena have been observed in the adsorption of phosphorous on calcined alunite [42], Fe(III)/Cr(III) hydroxide [43], and ion exchange fiber [44].

3.6. Effect of adsorption temperature and phosphate adsorption isotherm

The results of phosphate adsorption isotherm experiments at 25, 35, 45, and 55°C are shown in Fig. 9. The adsorption capacity obviously increased as the temperature rose from 25 to 55°C. The observed enhancement in the adsorption capacity with an increase of the temperature indicates that the adsorption process is endothermic in nature. So the high temperatures favor phosphate removal by adsorption onto LGIOWP. This may be due to a tendency for the phosphate ions to react with the adsorbent more quickly with an increase in temperature of the solution. This effect suggests that an explanation of the adsorption mechanism associated with the removal of phosphate onto LGIOWP involves a chemisorption process in this case.

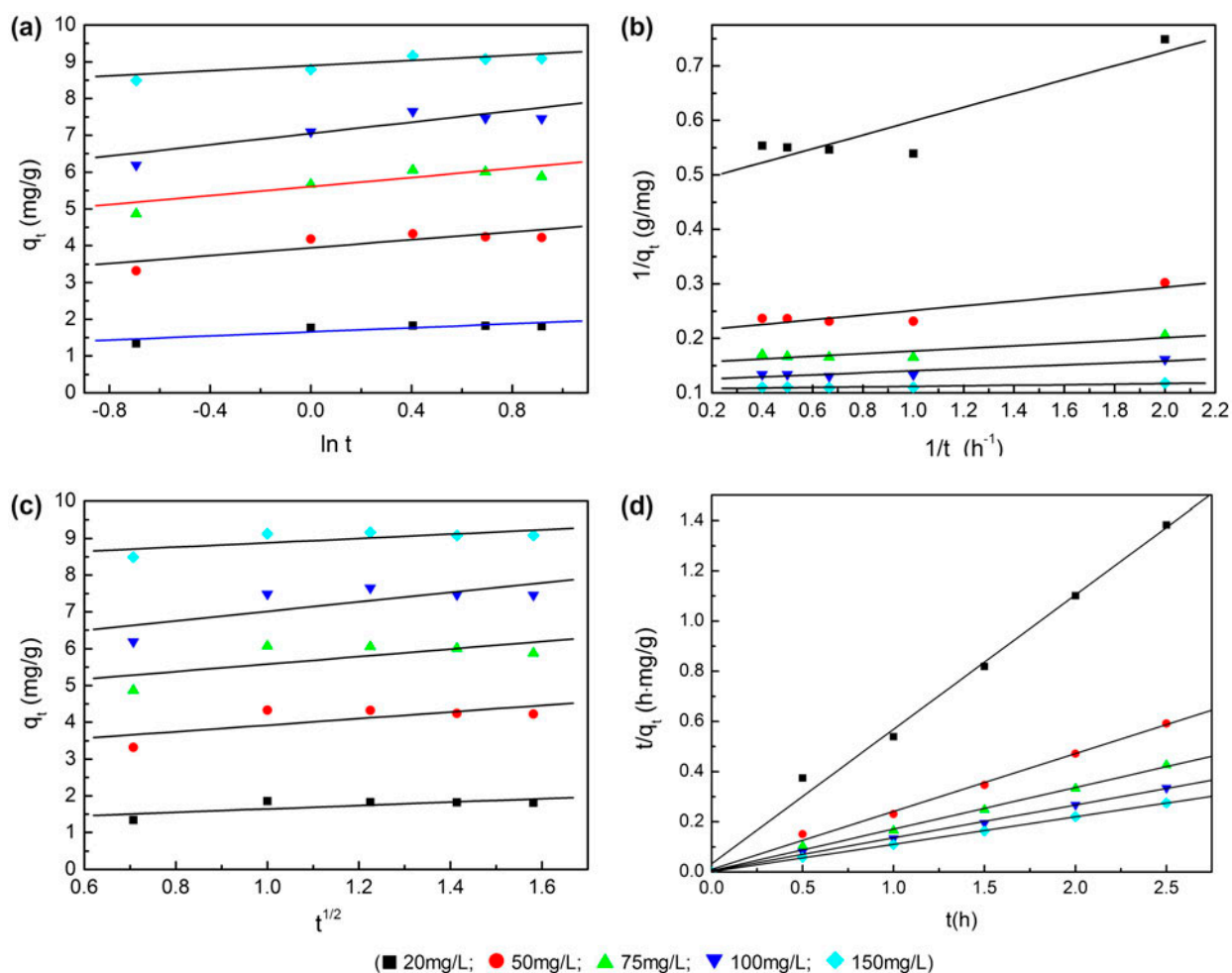


Fig. 8. Linearized form plot of kinetic model for phosphate adsorption on LGIOWP. (a) Elovich model; (b) pseudo-first-order model; (c) intra-particle diffusion model; and (d) pseudo-second-order model.

Table 1
Estimated kinetic model parameters for phosphate adsorption on LGIOWP

Elovich model: $q_t = \frac{1}{\beta \ln(\alpha\beta)} + \frac{1}{\beta} \ln t$				
Initial phosphate concentration (mg/L)	α (mg/(g·min))	β (g/mg)	R^2	SD
20	0.3262	3.6219	0.6337	0.1540
50	0.6130	1.8685	0.6144	0.3111
75	0.6881	1.6221	0.5841	0.3817
100	0.8559	1.3028	0.6661	0.3989
150	0.3647	2.8523	0.6401	0.1929
Pseudo-first-order model: $\frac{1}{q_t} = \frac{k_1}{q_e t} + \frac{1}{q_e}$				
Initial phosphate concentration (mg/L)	k_1 (min ⁻¹)	q_e (mg/g)	R^2	SD
20	0.2693	2.1205	0.8354	0.0422
50	0.2047	4.8001	0.8231	0.0148
75	0.1585	6.5587	0.8020	0.0090
100	0.1493	8.1940	0.8550	0.0056
150	0.0473	9.3694	0.8300	0.0017
Intra-particle diffusion model: $q_t = c + k_m t^{1/2}$				
Initial phosphate concentration (mg/L)	c	k_m (mg/(g·min ^{1/2}))	R^2	SD
20	1.1790	0.4640	0.5246	0.1755
50	3.0266	0.8942	0.5029	0.3533
75	4.5602	1.0212	0.4699	0.4310
100	5.7216	1.2932	0.5542	0.4609
150	8.2911	0.5886	0.5289	0.2207
Pseudo-second-order model: $\frac{t}{q_t} = \frac{1}{k_2 q_e^2} + \frac{t}{q_e}$				
Initial phosphate concentration (mg/L)	k_2 (g/(mg·min))	q_e (mg/g)	R^2	SD
20	8.6516	1.8667	0.9969	0.0440
50	5.1522	4.3346	0.9980	0.0154
75	5.4072	6.0277	0.9985	0.0096
100	3.6916	7.6161	0.9989	0.0066
150	9.6519	9.1408	0.9999	0.0019

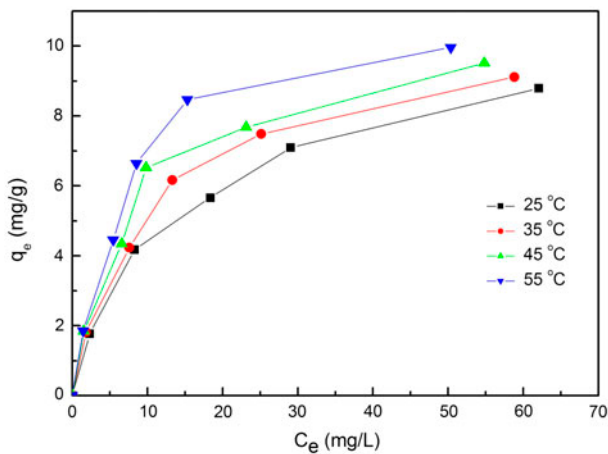


Fig. 9. Adsorption isotherm of phosphate by LGIOWP at different temperatures.

In order to further investigate the behavior of phosphate adsorption on LGIOWP, the isotherm data from Fig. 10 were fitted to Langmuir and Freundlich

equations (Eqs. (7) and (8)). The fitted Langmuir and Freundlich plots are shown in Fig. 10(a) and (b), respectively, along with the experimental data. The correlation coefficient (R^2) and the standard error of estimate (SD) using different isotherm equations are listed as Table 2. It can be seen from Table 2, the R^2 values indicate that Langmuir plots are better fitted with the experimental data as compared to the Freundlich plots. So the isotherm of phosphate adsorption on the LGIOWP obeys the Langmuir equations. The trend also suggests that chemisorption maybe the main adsorption mechanism in the system.

Compared to most of the other low-cost adsorbents with similar component, LGIOWP exhibits enhanced capacity for phosphate adsorption at ambient temperatures. As seen from Table 3, for adsorption temperature 55 °C, an adsorbent dosage of 10 g/L, at pH 5.6, adsorption 1 h, and initial phosphate concentration 20–150 mg/L, the value of the maximum adsorption capacity (q_{max}) was found to be 11.44 mg/g. The adsorption capacity of LGIOWP is about 67 times of

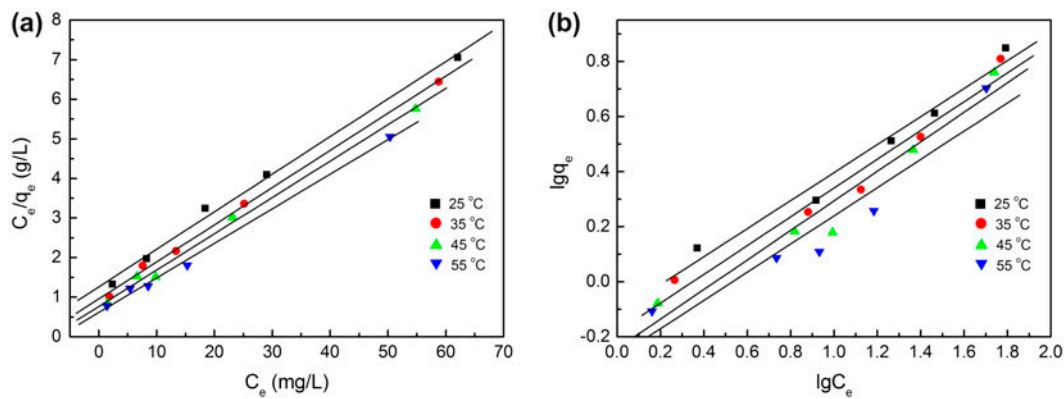


Fig. 10. Linearized form plot of isotherm for phosphate adsorption on LGIOWP. (a) Langmuir isotherm and (b) Freundlich isotherm.

Table 2
Estimated isotherm parameters for phosphate adsorption on LGIOWP

Temperature (°C)	Langmuir isotherm $\frac{C_e}{q_e} = \frac{C_e}{q_{\max}} + \frac{1}{K_L q_{\max}}$				Freundlich isotherm $\lg q_e = \lg K_F + \frac{\lg C_e}{n}$			
	K_L (L/g)	q_{\max} (mg/g)	R^2	SD	K_F ($\text{mg}^{1-1/n} \text{L}^{1/n}$)	$1/n$	R^2	SD
25	0.0753	10.54	0.9945	0.1836	0.7712	0.5088	0.9724	0.0540
35	0.0987	10.65	0.9986	0.1050	0.6566	0.5226	0.9640	0.0660
45	0.1198	10.90	0.9956	0.1518	0.5711	0.5364	0.9481	0.0848
55	0.1427	11.44	0.9961	0.1251	0.5328	0.5125	0.9108	0.1051

Table 3
Phosphate adsorption conditions and capacities of different natural adsorbents

Sl. no.	Material	Initial phosphate concentration (mg/L)	pH	Adsorption capacity (mg/g)	References
1	Phosphate mine slimes	50	7.0	5.63	[18]
2	Iron oxide tailings	5–150	6.6	8.21	[11]
3	Dolomite	0–100	11.0	0.17	[16]
4	Limestone	5–25	8.6	0.30	[10]
5	Apatite	5–150	7.0	1.09	[20]
6	Natural zeolite	500–10,000	7.0	2.15	[21]
7	Blast furnace slag	50–500	7.0	18.90	[14]
8	Ferric sludge	5–50	5.5	25.50	[12]
9	Hematite	80.3–443.5	4.8–6.0	3.00	[9]
10	LGIOWP	20–150	5.6	11.44	This study

the adsorption capacity of dolomite [16], 4, 10, and 1.4 times of the adsorption capacity of hematite [9], apatite [20], and iron oxide tailings [11], respectively. So the results show that the LGIOWP could be considered as promising materials to remove phosphate. In addition, the exhausted LGIOWP adsorbed-phosphate product possess the value of further utilizing, as this product has a potential application to be used as a

raw material to produce P fertilizer due to the fact that P is enriched in the exhausted LGIOWP.

4. Conclusions

LGIOWP, a type of waste that contains mainly active mineral materials including hematite and dolomite, was used as an adsorbent to remove

phosphate from aqueous solution with phosphate. Effects of pH value, LGIOWP dosage, initial phosphate concentration, adsorption time, and adsorption temperature on phosphate removal efficiency were investigated. In addition, phosphate adsorption kinetics and adsorption isotherm were evaluated. Based on the results of this study, the following conclusions can be drawn.

- (1) The plot of adsorption efficiency of phosphate vs. pH value appears to the pattern “M.” When pH value is 5.6, the maximum phosphate removal capacity is obtained. Another phosphate removal capacity peak appears as the pH value is 10.67. Adsorption of phosphate mainly on hematite is likely the key mechanism for phosphate removal using the present LGIOWP at pH values ranging from 1 to 9. As pH value is above 9, dolomite play more important role in phosphate removal.
- (2) The adsorption capacity of LGIOWP increases with increase in the initial phosphate concentration. The adsorption saturation time was 1 h for all initial phosphate concentrations studied (20–150 mg/L). The optimal LGIOWP dosage was 10 g/L. The adsorption kinetics characteristics are well described by the pseudo-second-order kinetic model.
- (3) The adsorption capacity increases with increase in the adsorption temperature. The isotherm of phosphate adsorption on the LGIOWP at different temperatures can be satisfactorily described by the Langmuir equations. The trend suggests that chemisorption maybe the main adsorption mechanism in the system.
- (4) It is demonstrated that the LGIOWP are an effective adsorbent for phosphate removal. Due to their low cost and high capability, the LGIOWP have the potential to be utilized for cost-effective removal of phosphate from aqueous solution.

Acknowledgments

This work was financially supported by the National Natural Science Foundation of China (grant 51174246). Authors are grateful to the editors and anonymous reviewers for their helpful suggestions and enlightening comments.

References

- [1] E. Valsami-Jones, Mineralogical controls on phosphorus recovery from wastewaters, *Mineral. Mag.* 65 (2001) 611–620.
- [2] Y. Comeau, K.J. Hall, R.E.W. Hancock, W.K. Oldham, Biochemical model for enhanced biological phosphorus removal, *Water Res.* 20 (1986) 1511–1521.
- [3] S. Tsuneda, T. Ohno, K. Soejima, A. Hirata, Simultaneous nitrogen and phosphorus removal using denitrifying phosphate-accumulating organisms in a sequencing batch reactor, *Biochem. Eng. J.* 27 (2006) 191–196.
- [4] T. Clark, T. Stephenson, P.A. Pearce, Phosphorus removal by chemical precipitation in a biological aerated filter, *Water Res.* 31 (1997) 2557–2563.
- [5] S.L. Tian, P.R. Jiang, P. Ning, Y.H. Su, Enhanced adsorption removal of phosphate from water by mixed lanthanum/aluminum pillared montmorillonite, *Chem. Eng. J.* 151 (2009) 141–148.
- [6] Z. Geng, E.K. Hall, P.R. Berube, Membrane fouling mechanisms of a membrane enhanced biological phosphorus removal process, *J. Membr. Sci.* 296 (2007) 93–101.
- [7] L.M. Blaney, S. Ginar, A.S. Gupta, Hybrid anion exchanger for trace phosphate removal from water and wastewater, *Water Res.* 41 (2007) 1603–1613.
- [8] M. Ozacar, Adsorption of phosphate from aqueous solution onto alunite, *Chemosphere* 51 (2003) 321–327.
- [9] A. Dimirikov, A. Joannou, M. Doula, Preparation, characterization and sorption properties of hematite, bentonite and bentonite-hematite systems, *Adv. Colloid Interface Sci.* 97 (2002) 37–61.
- [10] L. Johansson, Industrial by-products and natural substrata as phosphorus sorbents, *Environ. Technol.* 20 (1999) 309–316.
- [11] L. Zeng, X.M. Li, J.D. Liu, Adsorptive removal of phosphate from aqueous solutions using iron oxide tailings, *Water Res.* 38 (2004) 1318–1326.
- [12] X. Song, Y. Pan, Q. Wu, Z. Cheng, W. Ma, Phosphate removal from aqueous solutions by adsorption using ferric sludge, *Desalination* 280 (2011) 384–390.
- [13] H. Zeng, B. Fisher, D.E. Giammar, Individual and competitive adsorption of arsenate and phosphate to a high-surface-area iron oxide-based sorbent, *Environ. Sci. Technol.* 42 (2008) 147–152.
- [14] B. Kostura, H. Kulveitova, J. Lesko, Blast furnace slags as sorbents of phosphate from water solutions, *Water Res.* 39 (2005) 1795–1802.
- [15] E.W. Shin, J.S. Han, M. Jang, S.H. Min, J.K. Park, R.M. Rowell, Phosphate adsorption on aluminum-impregnated mesoporous silicates: Surface structure and behavior of adsorbents, *Environ. Sci. Technol.* 38 (2004) 912–917.
- [16] S. Karaca, A. Gurses, M. Ejder, M. Acikyildiz, Adsorptive removal of phosphate from aqueous solutions using raw and calcinated dolomite, *J. Hazard. Mater.* 128 (2006) 273–279.
- [17] K.H. Goh, T.T. Lim, Z.L. Dong, Application of layered double hydroxides for removal of oxyanions: A review, *Water Res.* 42 (2008) 1343–1368.
- [18] S. Jellali, M.A. Wahab, M. Anane, K. Riahi, L. Boussemli, Phosphate mine wastes reuse for phosphorus removal from aqueous solutions under dynamic conditions, *J. Hazard. Mater.* 184 (2010) 226–233.
- [19] K. Karageorgiou, M. Paschalis, G.N. Anastassakis, Removal of phosphate species from solution by adsorption on calcite used natural adsorbent, *J. Hazard. Mater.* 139 (2007) 447–452.

- [20] P. Molle, A. Lienard, A. Grasmick, A. Iwema, A. Kabbabi, Apatite as an interesting seed to remove phosphorus from wastewater in constructed wetlands, *Water Sci. Technol.* 51 (2005) 193–203.
- [21] K. Sakadevan, H.J. Bavor, Phosphate adsorption characteristics of soils, slags and zeolite to be used as substrates in constructed wetland systems, *Water Res.* 32 (1998) 393–399.
- [22] W. Xia, Z. Ren, Y. Gao, Removal of phosphorus from high phosphorus iron ores by selective HCl leaching method, *J. Iron Steel Res. Int.* 18 (2011) 1–4.
- [23] Y.S. Ho, G. McKay, Sorption of dye from aqueous solution by peat, *Chem. Eng. J.* 70 (1998) 115–124.
- [24] Y.S. Ho, G. McKay, Kinetic models for the sorption of dye from aqueous solution by wood, *Process Saf. Environ. Prot.* 76 (1998) 183–191.
- [25] D.L. Sparks. *Kinetics of Soil Chemical Processes*, Academic Press, San Diego, CA, 1989.
- [26] W.J. Weber Jr., J.C. Morris, Kinetics of adsorption on carbon from solution, *J. Saint. Eng. Div.* 89 (1963) 31–60.
- [27] I. Langmuir, The adsorption of gases on plane surfaces of glass, mica and platinum, *J. Am. Chem. Soc.* 40 (1918) 1361–1403.
- [28] H.M.F. Freundlich, Über die adsorption in lösungen [Over the adsorption in solution], *Z. Phys. Chem. (Leipzig)* 57(A) (1906) 385–470.
- [29] X. Song, Y. Pan, Q. Wu, Z. Cheng, W. Ma, Phosphate removal from aqueous solutions by adsorption using ferric sludge, *Desalination* 280 (2011) 384–390.
- [30] M.Y. Cana, E. Yildiz, Phosphate removal from water by fly ash: Factorial experimental design, *J. Hazard. Mater.* 135 (2006) 165–170.
- [31] R. Liu, J. Guo, H. Tang, Adsorption of fluoride, phosphate, and arsenate ions on a new type of ion exchange fiber, *J. Colloid Interface Sci.* 248 (2002) 268–274.
- [32] D.G. Drubb, M.S. Guimaraes, R. Valencia, Phosphate immobilization using an acidic type F fly ash, *J. Hazard. Mater.* 76 (2000) 217–236.
- [33] G. Sposito, *The Surface Chemistry of Soils*. Oxford University Press, New York, NY, 1984, p. 234.
- [34] A. Ringbom, *Complexation in Analytical Chemistry*. Interscience Publishers, New York, NY, 1963.
- [35] P. Ning, H.J. Bark, B. Li, X. Lu, Y. Zhang, Phosphate removal from wastewater by model-La (III) zeolite adsorbents, *J. Environ. Sci.* 20 (2008) 670–674.
- [36] L.G. Yan, Y.Y. Xu, H.Q. Yu, X.D. Xin, Q. Wei, B. Du, Adsorption of phosphate from aqueous solution by hydroxyl-aluminum, hydroxy-iron and hydroxy-iron-aluminum pillared bentonites, *J. Hazard. Mater.* 179 (2010) 244–250.
- [37] T. Liu, K. Wu, L. Zeng, Removal of phosphorus by a composite metal oxide adsorbent derived from manganese ore tailings, *J. Hazard. Mater.* 217–218 (2012) 29–35.
- [38] F. Arias, T.K. Sen, Removal of zinc metal ion (Zn^{2+}) from its aqueous solution by kaolin clay mineral: A kinetic and equilibrium study, *Colloids Surf. A* 348 (2009) 100–108.
- [39] T.K. Sen, M.V. Sarzali, Removal of cadmium metal ion (Cd^{2+}) from its aqueous solution by aluminum oxide (Al_2O_3): A kinetic and equilibrium study, *Chem. Eng. J.* 142 (2008) 256–262.
- [40] M.X. Loukidou, A.I. Zouboulis, T.D. Karapantsios, K.A. Matis, Equilibrium and kinetic modeling of chromium (VI) biosorption by *Aeromonas caviae*, *Colloids Surf. A* 242 (2004) 93–104.
- [41] M.C. Basso, E.G. Cerrella, A.L. Cukierman, Empleo de algas marinas para la biosorción de metales pesados de aguas contaminadas [Use of marine seaweed for the biosorption of heavy metals from contaminated water], *Avances en Energías Renovables y Medio Ambiente [Prog. Renew. Energies Environ.]* 6 (2002) 69–74 (in Spanish).
- [42] M. Ozacar, Equilibrium and kinetic modeling of adsorption of phosphorous on calcined alunite. *Adsorption* 9 (2003) 125–132.
- [43] C. Namasivayam, K. Prathap, Recycling Fe(III)/Cr(III) hydroxide, an industrial solid waste for the removal of phosphate from water, *J. Hazard. Mater.* 123 (2005) 127–134.
- [44] R.X. Liu, J.L. Guo, H.X. Tang, Adsorption of fluoride, phosphate and arsenate ions on a new type of ion exchange fiber, *J. Colloid Interface Sci.* 248 (2002) 268–274.